

Next-CSP Concept with Particle Receiver Applied to a 150 MW_e Solar Tower

Frédéric Siros^{1, a)}, Benoît Valentin^{1, b)}, Bo Liu¹, Jan Baeyens²,
and Gilles Flamant³

¹ Research Engineer, EDF R&D, 6 quai Watier 78400 Chatou - France

² European Powder and Process Technology, Park Tremeland 9, 3120 Tremelo, Belgium

³ PROMES-CNRS, Rue du Four Solaire 7, 66120 Font Romeu, France

^{a)}Corresponding author: frederic.siros@edf.fr

^{b)}benoit.valentin@edf.fr

Abstract. The current benchmark for CSP is the molten salt tower. The next generation of CSP plant should keep the general architecture of the current benchmark – namely the molten salt tower with its direct storage – but should operate at higher temperatures in order to downsize its solar field through higher efficiency. Solid particles are the best candidate today to replace the molten salt as storage medium.

Next-CSP is a project funded by the European Union's H2020 program that aims at developing a new concept of particle solar receiver and validating it with a 1.2 MW_e demonstration plant. The project also includes the study of a future utility-scale plant based on the concept in order to assess its technical and economic feasibility. This paper outlines the preliminary design of such a 150 MW_e Next-CSP plant. Costs were considered to make design choices but are not dealt with in this paper.

The plant is designed as a peaker that generates power during the evening. Due to inherent limitations of the concept, the solar receiver is a cavity one with a limited thermal output, which makes a multi-tower configuration mandatory. Our plant has six towers, each one with one receiver. Bucket elevators were chosen to lift the particles from ground level to the receivers. The layout of the whole solar island was optimized to minimize the cumulated length of the network that horizontally conveys the particles between the storage system and the six towers. The chosen layout, named “Vertical Star”, allows for a cumulated length of 4.0 km, which is still very challenging in terms of Capex and thermal losses. Continuous-flow conveyors and proper design limit the thermal losses to 5%.

The power cycle is an externally-heated gas turbine operated in combined cycle. Whilst the bottoming steam cycle is standard, the gas turbine features a double reheat in order to achieve a combined cycle efficiency approaching 50%. The heat exchangers that provide the heat from the particles to the gas turbine are numerous (ten) and bulky.

To conclude, the deployment of a utility-scale Next-CSP plant can realistically be envisioned; however, some technical challenges must be dealt with carefully, especially the thermal losses of the solar receiver and the particle conveying network.

INTRODUCTION

Objective of the Study – Outline and Scope of this Paper

The Next-CSP project aims at developing a demonstration 1.2 MW_e Concentrated Solar Power plant that uses solid particles as both heat transfer fluid and storage medium. The project also paves the way towards commercial developments of this technology by studying its scale-up to industrial size. This paper outlines the preliminary design of a typical 150 MW_e plant to be built around 2030. Unlike the current demonstration plant whose gas turbine is operated with a supplementary firing (needed by the solarized OPRA OP16 turbine in order to reach its design Turbine Inlet Temperature of about 1000°C), the utility-scale plant envisioned is 100% solar. The plant has the same general architecture as that of a molten salt tower. The core novel concept of Next-CSP is the receiver technology –

namely, the in-tube upward bubbling fluidized bed (UBFB) of particles. Other major innovations involve the whole solar loop (that includes the receiver, the storage system and all the devices that convey the particles between both) as well as the power cycle. Some parts of the plant (e.g. the heliostats) do not differ inherently from those of our benchmark (i.e. the molten salt solar tower) and need not be described in this document; conversely, special emphasis is placed on the most innovative parts of the plant.

SOLAR ISLAND

Dispatch Strategy Chosen

The areas where CSP is deployed are well-irradiated and (in most cases) hot during the day; air conditioning represents a big (and increasing) share of the consumption and photovoltaic (that accounts for most of the non-flexible power generation wherever CSP is built) is growing. Therefore, in the mid-term future, the net load (demand minus non-flexible production) of these electric systems will peak steeply during the afternoon. This is shown clearly by the famous “duck curve” of California that offers generally a good predictive picture of what will happen next elsewhere.

Considering the above, the scaled-up plant is designed to be operated as a peaker. Power generation starts a little before sunset and ramps up linearly until it reaches full load (150 MW_e) 40 minutes later; full load is then kept during 4 hours and 20 minutes; eventually, load decreases linearly down to zero in 40 minutes. This corresponds to 5 full load equivalent hours of power generation. With proper design, the load variations (from zero to full load and vice-versa in 40 minutes each) are feasible for our 150 MW_e power cycle.

With a nominal efficiency of the power cycle of 48.6% in nominal conditions and about 40% during the transients, one can determine that the daily heat consumption of the power cycle is about 1.6 GW_{th}.

Geometry and Sizing of the Solar Receiver

Cavity Receiver Mandatory to Mitigate Heat Losses

The thermal losses of external molten salt receivers range from 5% to 10%. Except when strong winds cause significant forced convection, most of these losses are radiant. In order to assess the temperature of the external wall of the receiver tubes, the following assumptions were made regarding both a typical molten salt receiver and our UBFB receiver:

Molten salt receiver

- Tube material: Inconel®625. Conductivity $\lambda = 15.3$ W/m/K for $T = 400^\circ\text{C}$; $\lambda = 18.3$ W/m/K for $T = 600^\circ\text{C}$
- Tube thickness = 2 mm
- Fouling factor = 9.10^{-5} m².K/W
- Molten salt entering the receiver at 290°C and exiting it at 565°C
- Net incoming flux Φ decreasing with salt bulk temperature (T_{salt}):
 $\Phi = 800$ kW/m² where $T_{salt} = 290^\circ\text{C}$ and $\Phi = 300$ kW/m² where $T_{salt} = 565^\circ\text{C}$

Considering the above, the external wall temperature of the receiver tubes ranges from ~525°C to ~650°C.

UBFB receiver

Calculations were made to extrapolate the experimental results to the operating conditions of the scaled-up receiver: tubes in high-grade Nickel-based superalloy, average net incoming flux ~550kW/m², same tube thickness and fouling factor as above. Particles are fed at 600°C to the bottom of the UBFB tubes and disengaged from their top at 825 °C. In view of these considerations, one can reasonably assume that the external wall temperature of the tubes will range from ~900°C (at the bottom of the tubes) to ~1050°C (at their top).

Comparison of the thermal losses of both receivers

Most of the losses are radiant and proportional to T^4 where T is the absolute temperature; the irradiated area of both receivers are similar as are the net average incoming fluxes: about 550kW/m². All else being equal, the radiant losses of the receiver are roughly proportional to the “exponent four-weighted mean temperatures”. Consequently, the thermal losses of the UBFB receiver are about 4 times those of a corresponding molten salt receiver. Such extra

losses are of course unacceptable since they would offset or even exceed the gain in power cycle efficiency that is (along with cheaper storage) the main objective of the UBFB technology.

The outcome of this quick analysis is clear: only a cavity receiver is suitable to the UBFB technology.

Limited Maximum Power Output of the Solar Receiver

The irradiated height of the tubes is limited to 8.0 m in order to keep a safety margin regarding hydrodynamic limitations (slugging and reduced wall-to-bed heat transfer) in the highest part of the tubes.

Vertically stacking several rows of tubes in the receiver should be feasible, but would lead to a rather complex receiver design with a lot of extra hardware. Therefore, the height of the irradiated area is 8.0 m.

The width of the irradiated area is 13.0 m. The corresponding width/height ratio of ~ 1.63 limits the spillage while using heliostats with standard size and good accuracy. These considerations limit the irradiated area of the receiver to 104 m^2 ($H \cdot L = 8.0 \cdot 13.0$). A net incoming flux of about 540 kW/m^2 (close to the maximum allowable flux) corresponds to a receiver output of $56.2 \text{ MW}_{\text{th}}$.

These characteristics may be altered in the future: further studies, optimization and testing are ongoing. However, the accuracy of the abovementioned figures is sufficient at this stage of preliminary design.

Optimal Thermal Power of the Solar Island – Number of Solar Receivers

Simulations were made using the System Advisor Model (SAM) software tool developed by NREL. The site considered is Ouarzazate, Morocco, with a yearly DNI of $2635 \text{ kW/m}^2 \cdot \text{year}$ and a latitude of 31° . These are typical conditions for CSP. The main results were as follows:

1. One $56.2 \text{ MW}_{\text{th}}$ receiver collects $99.250 \text{ GWh}_{\text{th}}$ per year;
2. The receiver collects $280 \text{ MWh}_{\text{th}}$ during the day ranked 217th by decreasing heat collection (in other words, $\sim 40\%$ of the 365 days are worse and $\sim 60\%$ are better).

As explained before, the power cycle needs a daily heat input of $1.60 \text{ GWh}_{\text{th}}$ to meet the dispatch requirements. In practice, about $1.68 \text{ GWh}_{\text{th}}$ must be collected daily by the solar receivers, taking into account various heat losses accounting for $\sim 5\%$.

3. According to 1. above, six solar receivers collect $595,500 \text{ MWh}_{\text{th}}$ per year. Therefore, should the thermal storage be unlimited in size and able to release the heat after several months without any loss, these six receivers would fully meet the dispatch requirement 354 days per year ($595,500 \cdot 6 / 1,680 = 354.5$).
4. According to 2. above, six solar receivers collect at least the required daily amount of heat ($1.680 \text{ GWh}_{\text{th}}$) during 217 days per year. Therefore, should the thermal storage be limited to 24 hours (thus requiring the heat collected during a day to be entirely discharged for power generation during the following evening), these six receivers would fully meet the dispatch requirement 217 days per year.

The reality lies somewhere between hypotheses 3. and 4. above (respectively too pessimistic and too optimistic). Further simulations showed that six receivers should allow the plant to fully meet the dispatch requirement during about 280 days per year and help the electric grid with partial peak production during about 40 days a year.

In conclusion, six solar receivers are considered for our plant, at least at the preliminary stage of plant design.

SIZING OF THE THERMAL STORAGE SYSTEM

Since power generation must be avoided during daytime, the sizing of the storage must correspond to a whole day of thermal collection minus the heat consumption of power cycle start-up that overlaps with solar collection. It is a trade-off: a storage sized for a clear 21st June would rarely be fully charged whereas a storage sized for a clear 21st December would cause frequent curtailment of the solar field. Since the solar field is costlier than the thermal storage system, the optimum is closer to the first scenario; we chose to size the storage for the heat collected during the $\sim 90^{\text{th}}$ best day of the year (i.e. corresponding to the first quartile of daily heat collection). During such a day, $2,240 \text{ MWh}_{\text{th}}$ (about 6.6 full load-equivalent hours of heat collection) are collected by the six receivers. Taking the 5% heat losses caused by particle handling and particle-to-air heat exchangers, $2,130 \text{ MW}_{\text{th}}$ are provided to the thermal storage during that day.

The heat consumption of the power cycle during the ramp-up period corresponds to 1/3 hour of full load power generation with an overall efficiency of about 40%: $150 \cdot (1/3) / 0.40 = 125 \text{ MWh}_{\text{th}}$. It is discharged during the end

of the heat collection. Therefore, the required capacity of the storage system is $2,130 \text{ MWh}_{\text{th}} - 125 \text{ MWh}_{\text{th}}$, or about $2.0 \text{ GWh}_{\text{th}}$.

Considering 1/ the temperature difference of the storage: 200 K ; 2/ the specific heat capacity and the bulk density of olivine at 700°C (the heat is gained and released between $\sim 600^\circ\text{C}$ and $\sim 800^\circ\text{C}$): 1.22 kJ/kg/K and $\sim 2000 \text{ kg/m}^3$; the mass and volume of olivine contained by the storage system are $30,000 \text{ tons}$ and $15,000 \text{ m}^3$.

Four hoppers (two cold + two hot) are used, each hopper containing 7500 m^3 of particles. They are cylindrical with an internal diameter of 30 m , a V-shaped bottom and a storage height of 16 m .

SOLAR FIELD

Main Characteristics of Each Solar Module

The whole solar field consists of six identical modules, one module including a tower, a cavity receiver on top of it and a solar field located north of the tower (for our plant that is built in the northern hemisphere). The tower height (from heliostats' mirror level to mid-height of the receiver's panel) is 126 m . The Stello[®] heliostat was developed by sbp GmbH (partner of Next-CSP) [4]; its mirror area is 48.5 m^2 . Each individual solar field includes $1,879$ heliostats; its shape corresponds roughly to an ellipse whose northernmost heliostats were removed, as shown in Fig. 1 below. This rather "wide" shape is well suited to the wide aperture of the receiver.

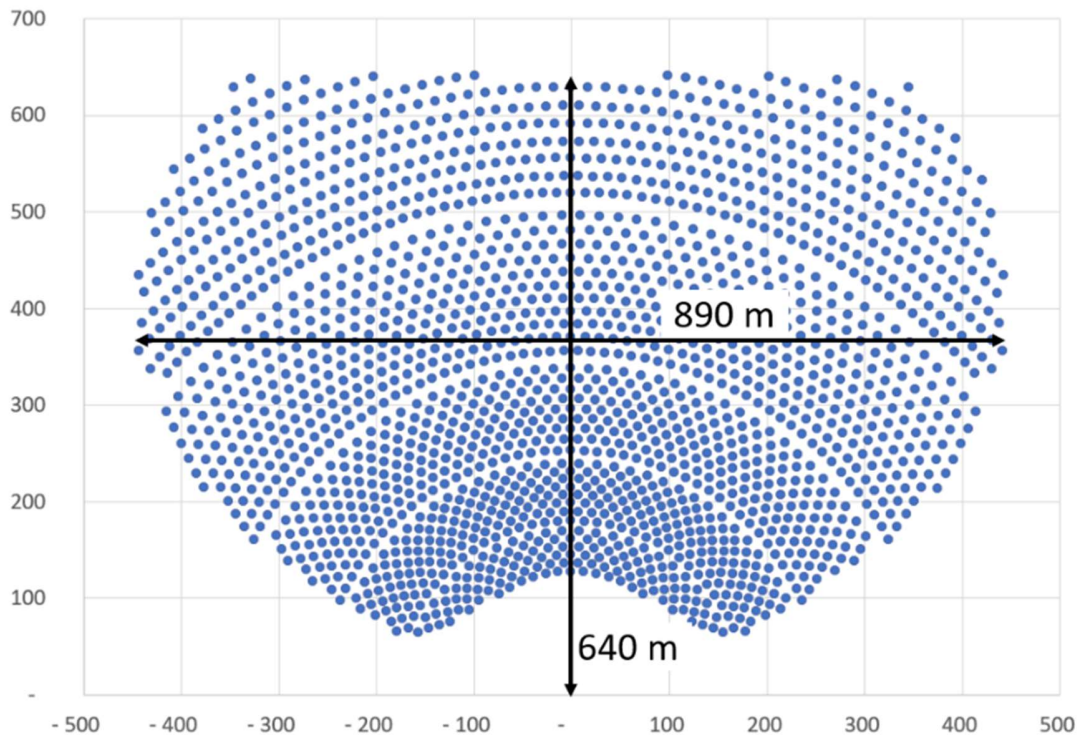


FIGURE 1. Layout of each individual solar field. Each dot represents a heliostat.

Due to the favorable geometry (north field with a proportionally high tower), the efficiency of the field is 80.6% . Our objective regarding the thermal efficiency of the receiver is 85% ; design optimization can be found in [5].

Layout of the Whole Solar Island

The particles must be conveyed horizontally between the storage system and the six towers. The corresponding thermal losses and extra Capex are roughly proportional to the cumulated length of the conveying. Various arrangements of the six solar modules were envisioned and compared, including those shown in Fig. 2 below:

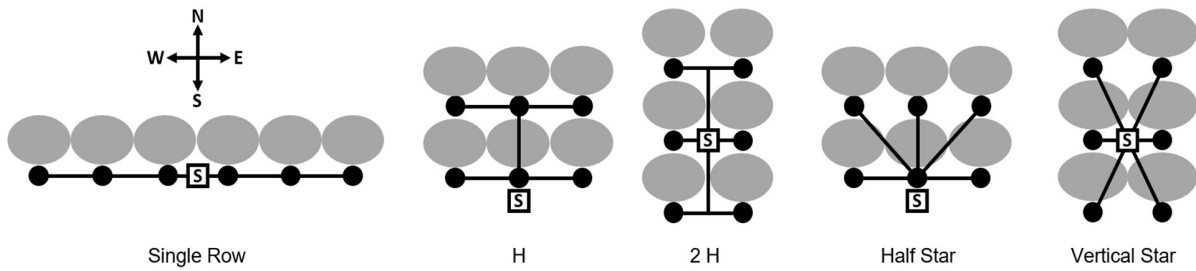


FIGURE 2. Layouts envisioned for the whole solar island. The black dots represent the towers, the grey ellipses represent the individual solar fields, the black lines represent the conveying paths and the box with an “S” represent the storage system.

The path lengths that convey a particle mass flow corresponding to two or three towers are accounted for 1.8 times and 2.8 times respectively. The Vertical Star arrangement allows for the lowest conveying cumulated length. Besides, once the Vertical Star arrangement is chosen, the shape of our individual solar fields (namely, their [North-South Length] / [East-West Width] ratio = $640 / 890 = 0.72$, as shown in Fig. 1 above) provides the minimum cumulated length for a given area of the solar field.

With the dimensions shown in Fig. 1 above for each individual solar field, the cumulated length of the particle conveying system is 4.0 kilometers. The capacity of each conveyor correspond to one tower and is approx. 220 kg/s.

PARTICLE HANDLING

In order to lift the particles from ground level to the receivers, skip hoists (derived from those used in the mining industry) were envisioned [6]. Bucket elevators were eventually chosen because their near-continuous operation allows reducing the buffer storage of particles located atop the tower. The bucket elevators must be designed to withstand temperatures of about 600°C and to mitigate the thermal losses; some manufacturers can meet these requirements. Given the particle mass flow and the tower height, several elevators in parallel and in series are probably required: 2 x 2 elevators per tower is the most likely configuration.

As explained above, the horizontal conveying of the particles between the storage system and the towers (from the storage system to the towers at $\sim 620^{\circ}\text{C}$ and in the opposite direction at $\sim 820^{\circ}\text{C}$) amounts to 4.0 km each way. Electric consumption is not critical because it takes place during the day and can therefore be provided by a small dedicated PV farm equipped with a buffer battery, which is rather cheap. On the other hand, the Capex and, above all, the thermal losses of the conveying technology are key criteria.

Automated railway wagons were first considered, then apron conveyors (Fig. 3a below). Eventually, further studies taking the abovementioned criteria into account led us to choose continuous-flow conveyors (Fig. 3b below).

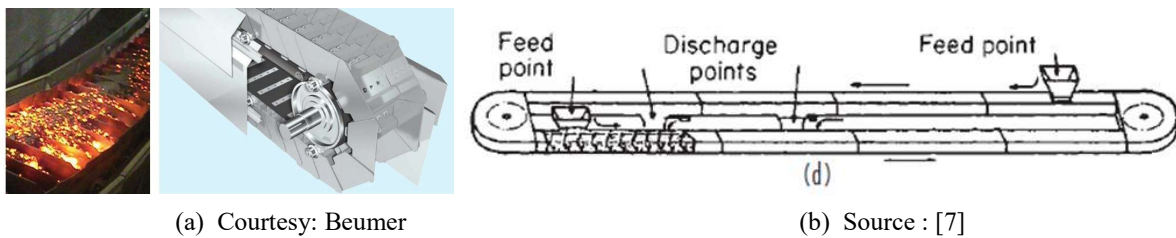


FIGURE 3. (a) Apron conveyors conveying materials at 600°C . | (b) Continuous-flow conveyors.

The Auxiliary power consumption and the thermal losses of the whole particle handling system were assessed considering bucket elevators and apron conveyors. The results were as follows:

- Power consumption: $\sim 2.5 \text{ MW}_e$. Since the gravitational energy due to the tower height represents the majority of it, it should be quite similar after replacing the apron conveyors with continuous-flow conveyors.
- Thermal losses: $\sim 17.6 \text{ MW}_{th}$, or about 5% of the heat delivered by the solar island. Such losses would offset a big chunk of the gain expected from the improved conversion efficiency of the power cycle, which is unacceptable. The replacement of the apron conveyors with continuous-flow conveyors and proper

engineering practices (along with performing a more accurate, hence less conservative assessment) will cut the thermal losses to about 2.5%, which is still significant.

POWER CYCLE

Main Characteristics of the Power Cycle

The power cycle is a combined cycle whose gas turbine is externally heated without any supplementary firing. The bottoming cycle is off-the-shelf: three pressure with reheat and an air-cooled condenser. The gas turbine works with a TIT (Turbine Inlet Temperature) that is limited by the particle temperature (about 820°C); the resulting TIT (780°C) is much lower than those allowed by internal combustion (up to ~1,600°C in state-of-the-art gas turbines). The gas turbine has a double reheat architecture which is mandatory to achieve a combined cycle efficiency close to 50% with such a TIT, as shown by previous studies [9][10]. Consequently, the set of particle-to-air heat exchangers that provides the heat input to the power block is split into three pressure levels: HP, IP and LP that heat the air exiting respectively the compressor, the first turbine section, and the second turbine section. This is shown in Fig. 4 below. The gross power output of the gas and steam turbines are 81 MW_e and 74 MW_e respectively, corresponding to a net power output of 150 MW_e for the power plant. The high pressure heat input (on the left side of Fig. 4) is 155.7 MW_{th}; the intermediate and low pressure heat inputs are 76.6 MW_{th} each.

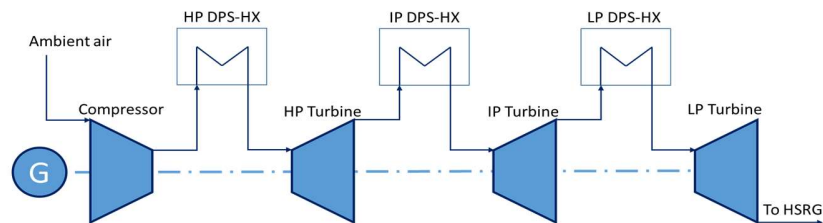


FIGURE 4. Externally heated gas turbine with double reheat

Particle-to-Air Heat Exchangers

Since they have a big impact on Brayton cycles' performances, the relative pressure drops of our heat exchangers must be limited to a few percent. The final temperature difference must also be minimized. Given the moderate air pressures, these combined requirements translate inevitably into bulky (and therefore costly) heat exchangers. The LP heat exchangers are obviously the most challenging ones in this regard. The exchangers are tube-and-shell with the air flowing through the tubes and the tubes immersed in the dense particle bed. Adequate air jets ensure proper fluidization of the particles and several baffles allow the heat exchangers to work in a quasi-counter-flow mode.

Considering the temperature of the particles exiting the solar receivers and the thermal losses affecting the conveying, the particles enter the heat exchangers at 820°C. Their average return temperature is 624°C. The average speed of the fluidization air is 0.05 m/s. The maximum heat losses affecting all heat exchangers of each pressure level is 0.8 MW_{th}, which amounts to 0.75% of the heat input for the whole set of heat exchangers (HP, IP and LP).

Due to the requirement of a large overall internal section area of the tubes (in order to limit the pressure drop through low air speed), several heat exchangers must be arranged in parallel for each pressure level: a single heat exchanger would otherwise be too wide relative to its length, thereby hampering proper particle circulation. There are respectively two HP, three IP and five LP heat exchangers in parallel.

The width of all exchangers is 2 m and the height of their particle bed is 3 m (corresponding to a somewhat higher shell); the length is 6 m for the HP and IP heat exchangers and 3 m for the LP heat exchangers.

Arrangement of the Power Island

The power house contains the turbomachinery which is single-shaft: gas turbine, generator, and steam turbine are on the same shaft oriented North-South. It also houses the ten particle-to-air heat exchangers, the corresponding piping, and the particle conveying network. The three IP and five LP heat exchangers are located respectively on the

east and west sides of the turbomachinery (or vice-versa); one of the two HP heat exchanger is located on the east side, the other on the west side. Since the sets of IP and LP heat exchangers have the same thermal power and return temperature (those of the HP heat exchangers being different), this arrangement ensures the same total thermal power of all the heat exchangers respectively located east and west of the turbomachinery (linked respectively to the east and west pairs – hot and cold – of particle hoppers).

Together, the ten heat exchangers represent a bigger land footprint than that of the turbomachinery, thereby resulting in a rather large power house: about 30 m x 30 m.

The Heat Recovery Steam Generator, the abovementioned power house and the air-cooled condenser are aligned (in this order) on a North-South axis. The area of the air-cooled condenser is about 2,400 m².

CONCLUSION – KEY TAKEWAYS

- The future design, construction and deployment of a utility-scale solar tower based on the Upward Bubbling Fluidized Bed concept developed in Next-CSP for the solar receiver are challenging but realistic;
- However, a cavity receiver is mandatory to mitigate heat losses, which limits the size of the solar field, thereby requiring a multi-tower architecture, along with several kilometers of horizontal particle conveying;
- The thermal losses of the solar receiver, the conveying network and the particle-to-air heat exchangers must be minimized;
- Besides the externally heated combined cycle gas turbine envisioned in this study, other highly efficient power cycles can be envisioned, including supercritical CO₂ Brayton or Rankine steam cycles.

ACKNOWLEDGMENTS

The Next-CSP project received funding from the European Union's Horizon 2020 research and innovation program under grant agreement No. 727762.

REFERENCES

1. D. Geldart, *Gas Fluidization Technology* - First Edition (Wiley, Hoboken, NJ, SA, 1987). ISBN 978-0471908067
2. H. Zhang, H. Benoit, D. Gauthier, J. Degève, J. Baeyens, I.P. López, M. Hemati, and G. Flamant, “Particle Circulation Loops in Solar Energy Capture and Storage: Gas–Solid Flow and Heat Transfer Considerations”, in *Applied Energy* 2016 161, 206-224. (Elsevier). DOI: <https://doi.org/10.1016/j.apenergy.2015.10.005>
3. H.L. Zhang, H. Benoit, I. Perez-Lopez, G. Flamant, T. Tan, and J. Baeyens, “High-Efficiency Solar Power Towers Using Particle Suspensions as Heat Carrier and in the Receiver and in the Thermal Energy Storage”, in *Renewable Energy*-2017 (Elsevier), 111, pp. 438-446. DOI: 10.1016/j.renene.2017.03.101
4. T. Keck, V. Schönfelder, B. Zwingmann, F. Gross, M. Balz, F. Siros, and G. Flamant, “High-Performance Stello Heliostat for High Temperature Application”, *SolarPACES 2020*
5. R. Gueguen, B. Grange, F. Bataille, S. Mer, and G. Flamant, “Shaping High Efficiency, High Temperature Cavity Tubular Solar Central Receivers”, in *Energies* (2020) 13, 4803. DOI:10.3390/en13184803
6. K. Repole and S. Jeter, “Design and Analysis of a High Temperature Particulate Hoist for Proposed Particle Heating Concentrator Solar Power Systems”, *ASME-2016*, DOI: 10.1115/ES2016-59619
7. R.H. Perry, D.W. Green, and J.O. Maloney, *Perry's Chemical Engineers' Handbook - 7th edition* (McGraw-Hill, New York, USA, 1997). ISBN 0-07-049841-5
8. H.I.H Saravanamuttoo, G.F.C Rogers, and H. Cohen, *Gas Turbine Theory - Fifth Edition* (Pearson Education Ltd., Harlow, UK, 2001). ISBN 10: 0-13-015847-X. ISBN 13: 978-0-13-015847-5
9. F. Siros and G. Fernández Campos, “Optimization of a Low-TIT Combined Cycle Gas Turbine with Application to New Generation Solar Thermal Power Plants”, in *ASME-2017*. Retrieved from: <http://proceedings.asmedigitalcollection.asme.org/proceeding.aspx?doi=10.1115/GT2017-65227>
10. B. Valentin, F. Siros, and J.F. Brau, “Optimization of a Decoupled Combined Cycle Gas Turbine Integrated in a Particle Receiver Solar Power Plant”, in *Proceedings of SolarPACES Conference, Casablanca, Morocco-2018*
11. I.E. Idel’Cik (translated from Russian by M. Meury), *Memento des pertes de charges* (Eyrolles, Paris, France). In French - Original Russian book published in Moscow in 1960